Asociación Argentina
de Mecánica Computacional

Mecánica Computacional Vol XXXIV, págs. 2225-2237 (artículo completo)
Sebastián Giusti, Martín Pucheta y Mario Storti (Eds.)
Córdoba, 8-11 Noviembre 2016

A VARIATIONAL CONTEXT FOR FSI SIMULATIONS INTRODUCING ARBITRARY BOUNDARY CONSTRAINTS

Andrés R. Valdez and Bernardo M. Rocha

Programa de Pós-Graduação em Modelagem Computacional, Universidade Federal de Juiz de Fora, Juiz de Fora, MG, Brazil, andres10valdez@gmail.com

Keywords: Variational principles; Navier Stokes; Arbitrary Boundary constraints; Lattice Boltzmann FSI solver

Abstract. We present a method for understanding Fluid Structure Interaction simulations in continuous media, an important class of phenomena that cover several fields of applications and research lines. Specialized literature has experienced a compelling need for improving the predictive skills of the models for simulations of fluid flow under arbitrary boundary conditions. In the present work, complex boundary conditions are those imposed by devious domains through where the fluid flows. We show a modeling procedure based on the Virtual Power Balance that results in a variational equation. The main consequence of this modeling procedure is the characterization of kinematic admissible loadings (stress-like and force-like loadings). Within the variational framework, we employ a numerical solver based on Lattice Boltzmann Method. The solver obtains the complete description of the desired phenomena like equilibrium conditions, constitutive equations, among other relevant features. Numerical experiments are presented to show the potential of the modeling procedure studied in this work to deal with several complex boundary constraints.

1 INTRODUCTION

When deriving a primal kinematic variational procedure for an arbitrary constrained model like Fluid Structure Interaction (FSI) phenomena, the mandatory principle for setting the basis, is the Principle of Virtual Power Balance, properly described in the research work of Germain (1973); Maugin (1980). If the context provides such conditions for writing the Principle of Virtual Power Balance, the characterization of generalized forces and generalized motion actions is obtained in a straight-forward manner as natural consequences. The characterization procedure is based on a duality of power when studying the interplay between powers' loads and motion actions. This duality allows the understanding of variational formulations as constrained minimization problems in which fluid flows embedded in complex domains.

Since the late 80's the Lattice Boltzmann Method (LBM) has undergone uncountable upgrades, allowing the community to perform efficient simulation of complex fluid dynamics in many different applications. Significant advances in computational hemodynamics have been shown in the research of Golbert et al. (2012); Artoli et al. (2004) and also in the work of Freund (2014), where the cellular detail of blood is an essential factor in its flow, especially in vessels or devices with size comparable to that of its suspended cells. It is within this context that we study the consequences of including obstacles in the flow.

This article is organized as follows: Section 2 presents the appropriate environment to develop with variational arguments, a dual balance principle for arbitrary challenging engineering situations; Section 3 assesses the modeling procedure exposed previously to model the fluid flow phenomena under arbitrary boundary constraints; Sections 4 and 5 expose the consequences of implementing the derived *Euler-Lagrange* equations when a Lattice Boltzmann Method is used for numerical simulations. To recall the pertinence of the modeling procedure, a bi-dimensional implementation is shown in Sections 6 and 7, where several relevant numerical experiments are presented. Finally, the concluding remarks are shown in Section 8.

2 VIRTUAL POWER BALANCE IN CONTINUUM MECHANICS

The physical modeling based on Virtual Power is one of the reliable modeling techniques in terms of including in the phenomena compatible loadings, as shown in Germain (1973); Maugin (1980) and Taroco et al. (2014). The *Virtual Power Balance* is going to be written as a fundamental principle, whose local and global consequences are established as follows.

Axiom 1 (Principle of Virtual Power Balance.) *Let a system Ω be in equilibrium with respect to a given Galilean frame; then, in any virtual motion, the virtual power of all the* ***internal forces*** *and* ***external forces*** *acting on Ω is null.*

The *Principle of Virtual Power Balance* can be finally written as

$$P_i(\mathbb{D}(\hat{\mathbf{u}})) + P_e(\hat{\mathbf{u}}) = -\langle \mathbb{T}; \mathbb{D}(\hat{\mathbf{u}}) \rangle + \langle \mathbf{f}; \hat{\mathbf{u}} \rangle = 0 \quad \forall\, \hat{\mathbf{u}} \in \mathrm{Var}\,\mathcal{U}, \tag{1}$$

where the

- Kinematic admissible manifold for generalized velocities and generalized strain rate tensors, are defined as:

$$\mathrm{Kin}\,\mathcal{U} = \{\, \mathbf{u} \in \mathcal{U} \equiv \mathbf{H}^m(\Omega) \;+\; extra\ constraints \},$$
$$\mathrm{Kin}\,\mathcal{W} = \{\, \mathbb{D}(\mathbf{u}) \in \mathcal{W} \equiv \mathbf{L}^m(\Omega) \};$$

- Kinematic admissible space for velocities variations:

$$\mathrm{Var}\,\mathcal{U} = \{\, \mathbf{u}_1 - \mathbf{u}_2 \in \mathrm{Var}\,\mathcal{U} \;:\, \mathbf{u}_1, \mathbf{u}_2 \in \mathrm{Kin}\,\mathcal{U} \,\}.$$

For this purpose the adjoint transformations are obtained when performing integration by parts of the internal power, then due to Riesz representation theorem, adjoint transformations are equivalently defined with:

$$\langle \mathbb{T}; \mathbb{D}(\hat{\mathbf{u}}) \rangle_{\mathcal{W}^* \times \mathcal{W}} = \langle \mathbb{D}^* \mathbb{T}; \hat{\mathbf{u}} \rangle_{\mathcal{U}^* \times \mathcal{U}} \,. \tag{2}$$

Within this context, the dual spaces $(\cdot)^*$ are defined when applying adjoint transformation for any arbitrary member in $(\cdot)$. A major conclusion from the previous statement is that the nature of internal and external power belongs to the same set, thus they can be manipulated equivalently. Figure 1 presents a schematic illustration to represent the duality between internal and external power.

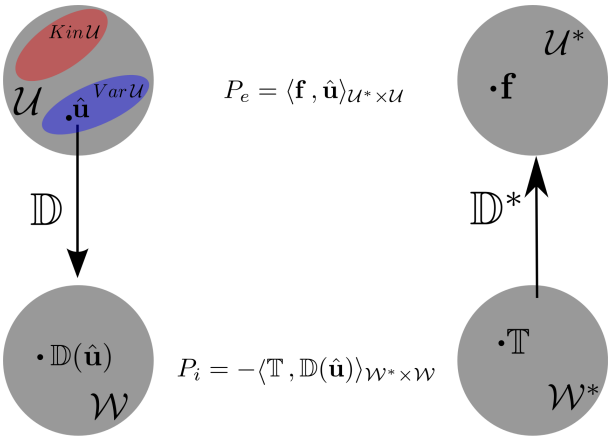

Figure 1: Schematic representation of duality in the Principle of Virtual Power.

Consider a loading system $\mathbf{f} = \{\mathbf{b}, \mathbf{t}\} \in \mathcal{U}^*$, as shown in Figure 2, where $\mathbf{t} \in \mathbf{L}^2(\partial\Omega_N)$ and $\mathbf{b} \in \mathbf{L}^2(\Omega)$ are loadings to be considered compatible with the model if the velocity field $\mathbf{u} \in \mathrm{Kin}\,\mathcal{U}$ satisfies

$$\int_\Omega (\mathbb{T}; \mathbb{D}(\hat{\mathbf{u}})) \; d\Omega = \int_\Omega (\mathbf{b}; \hat{\mathbf{u}}) \; d\Omega + \int_{\partial\Omega} (\mathbf{t}; \hat{\mathbf{u}}) \; d\partial\Omega \;, \forall\, \hat{\mathbf{u}} \in \mathrm{Var}\,\mathcal{U}; \tag{3}$$

where Cauchy's stress tensor is given by a particular constitutive law in terms of strain rate tensor such that $\mathbb{T}(\mathbf{u}) = \varphi(\mathbb{D}(\mathbf{u}))$.

The loadings given by $\mathbf{f} = \{\mathbf{b}, \mathbf{t}\}$ are uniquely characterized when integrating by parts the left hand side of Equation (3), that is

$$\int_\Omega (\mathbb{T}(\mathbf{u}); \mathbb{D}(\hat{\mathbf{u}})) \; d\Omega = -\int_\Omega (\mathrm{div}\,(\mathbb{T}(\mathbf{u})); \hat{\mathbf{u}}) \; d\Omega + \int_{\partial\Omega} (\mathbb{T}(\mathbf{u})\mathbf{n}; \hat{\mathbf{u}}) \; d\partial\Omega.$$

Thus, by replacing the previous expression in Equation (3) the loadings $\mathbf{f}$ can be defined as

$$\begin{cases} \mathrm{div}\,(\mathbb{T}(\mathbf{u})) + \mathbf{b} = 0, \;\; \text{in } \Omega, \\ \mathbb{T}(\mathbf{u})\mathbf{n} - \mathbf{t} = 0, \;\; \text{on } \partial\Omega_N. \end{cases}$$

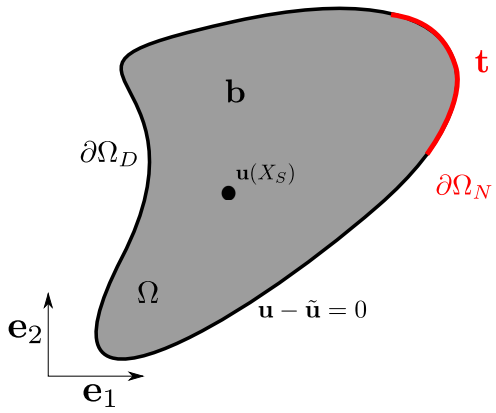

Figure 2: Generic motion actions and kinematic constraints acting over the domain, represented in a *spatial reference*.

3 VARIATIONAL APPROACH FOR INCOMPRESSIBLE NAVIER STOKES EQUATIONS

Navier Stokes equations are based on the analysis performed before, enhancing the Section 2, making special focus on the interplay between forces due to convective effects. Thus the following problem can be written:

Problem 2 (Navier Stokes equations) *Given a regular domain* Ω*, a source function* $\mathbf{f}$ *defined on* $\mathbf{L}^2(\Omega)$*, find the velocity field denoted by* $\mathbf{u}$*, defined on the following manifold*

$$\mathrm{Kin}\,\mathcal{U}^* \equiv \{\mathbf{w} \in \mathbf{H}^1(\Omega) : \mathbf{w}|_{\partial\Omega_D} = \mathbf{u}_D\},$$

and find the Lagrangian multiplier p *defined on the* $L^2(\Omega)$ *space, such that*

$$\begin{aligned}
&\int_\Omega \nu\,(\nabla\mathbf{u};\nabla\mathbf{v})\;d\Omega - \int_\Omega (\mathbf{f};\mathbf{v})\;d\Omega - \int_\Omega \eta_p\;\mathrm{div}\,(\mathbf{u})\;d\Omega - \int_\Omega p\;\mathrm{div}\,(\mathbf{v})\;d\Omega \\
&+ \int_\Omega \rho\;(\nabla\mathbf{u}\,\mathbf{u};\mathbf{v})\;d\Omega = 0, \\
&\forall\,(\mathbf{v},\eta_p) \in \left(\mathrm{Var}\,\mathcal{U}^*, L^2(\Omega)\right),
\end{aligned}$$

where the subspace $\mathrm{Var}\,\mathcal{U}^*$ *is defined as*

$$\mathrm{Var}\,\mathcal{U}^* = \{\,\mathbf{u}_1 - \mathbf{u}_2 \in \mathrm{Var}\,\mathcal{U}^* : \mathbf{u}_1, \mathbf{u}_2 \in \mathrm{Kin}\,\mathcal{U}^*\,\}.$$

Considering the region of the boundary with no Dirichlet boundary conditions, represented by $\partial\Omega_N = \partial\Omega \setminus \partial\Omega_D$ [1], and recalling that all admissible variations $\mathbf{v}$ vanish in the Dirichlet boundary $\partial\Omega_D$. Considering the use of Green's identity on the variational equations of Problem 2, the following expressions are obtained

$$\begin{aligned}
\int_\Omega \nu\,(\nabla\mathbf{u};\nabla\mathbf{v})\;d\Omega &= -\int_\Omega (\mathrm{div}\,(\nu\;\nabla\mathbf{u});\mathbf{v})\;d\Omega + \int_{\partial\Omega} ((\nu\;\nabla\mathbf{u})\,\mathbf{n};\mathbf{v})\;d\partial\Omega, \\
\int_\Omega p\;\mathrm{div}\,(\mathbf{v})\;d\Omega &= -\int_\Omega (\nabla p;\mathbf{v})\;d\Omega + \int_{\partial\Omega} (p\,\mathbf{n};\mathbf{v})\;d\partial\Omega,
\end{aligned}$$

[1] The complement of the Dirichlet's Boundary it is often called Neumann's Boundary, there was no reason to consider the Robin's Boundary condition, then it was neglected.

which upon substitution in the variational equations presented in Problem 2, yields the following Euler-Lagrange equations:

$$\begin{cases} -\operatorname{div}(\nu\ \nabla\mathbf{u}) - \mathbf{f} + \nabla p + \rho\ \nabla\mathbf{u}\,\mathbf{u} = 0, \quad \text{in } \Omega, \\ \operatorname{div}(\mathbf{u}) = 0, \quad \text{in } \Omega, \\ (\nu\ \nabla\mathbf{u} - p\,\mathbb{I})\ \mathbf{n} = 0, \quad \text{on } \partial\Omega_N, \\ \mathbf{u} - \mathbf{u}_D = 0 \quad \text{on } \partial\Omega_D. \end{cases} \tag{4}$$

3.1 Variational Equation for static obstructed fluid's flow

In fluid mechanics it is usual to have obstacles inside the regular domain Ω. Consider the case in which obstacles remains fixed and the no-slip condition is considered over its boundaries. In such cases, the obstacles introduces external forces which are the reactive forces to the no-slip conditions that the flow must comply. These reactive forces are put in evidence through the corresponding Lagrange multipliers. Considering that Γ^i, $i = 1, \cdots, N$[2] are the boundaries corresponding to the obstacles, Lagrange multipliers are denoted by $\gamma_i \in L^2(\Gamma^i)$. Figure 3 shows a description of the mentioned scenario, where the different domains are described.

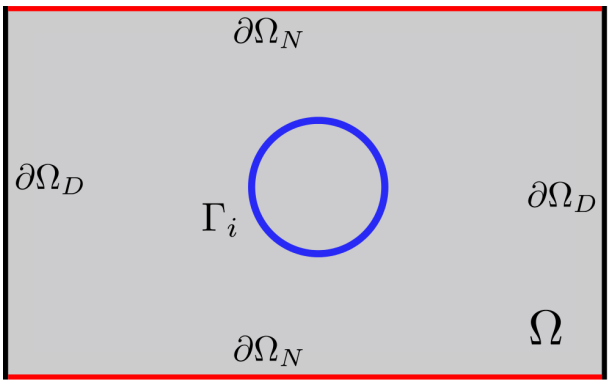

Figure 3: Schematic representation of an obstacle inclusion in the domain. Highlighted in red and black are the Neumann and Dirichlet boundary, respectively, whereas in blue the obstacles boundaries.

As a consequence of this new motion action, the Problem 2 must be rewritten. To address the changes due to obstacle inclusion the following problem is written:

Problem 3 (Navier Stokes equations with obstacles constraints) *Given a regular domain Ω, a source function $\mathbf{f}$ defined on $\mathbf{L}^2(\Omega)$, find the velocity field denoted by $\mathbf{u}$, defined over the following manifold*

$$\operatorname{Kin}\mathcal{U}^* \equiv \{\mathbf{w} \in \mathbf{H}^1(\Omega) : \mathbf{w}|_{\partial\Omega_D} = \mathbf{u}_D\},$$

and find the Lagrangian multipliers p and γ_i defined on $L^2(\Omega)$ and $L^2(\Gamma^i)$ spaces, respectively,

[2]Where N denotes the number of obstacles considered

such that

$$\int_\Omega \nu\,(\nabla \mathbf{u};\nabla \mathbf{v})\;d\Omega - \int_\Omega (\mathbf{f};\mathbf{v})\;d\Omega - \int_\Omega \eta_p\;\mathrm{div}\,(\mathbf{u})\;d\Omega - \int_\Omega p\;\mathrm{div}\,(\mathbf{v})\;d\Omega$$
$$+ \int_\Omega \rho\;(\nabla \mathbf{u}\,\mathbf{u};\mathbf{v})\;d\Omega + \sum_i^N \int_\Gamma (\gamma_i;\mathbf{v}) + (\eta_{\gamma_i};\mathbf{u}-\mathbf{u}_{slip})\;\mathrm{d}\Gamma = 0,$$
$$\forall\,(\mathbf{v},\eta_p,\eta_{\gamma_i}) \in \left(\mathrm{Var}\,\mathcal{U}^*, L^2(\Omega), L^2(\Gamma^i)\right),$$

where the subspace $\mathrm{Var}\,\mathcal{U}^*$ *is defined as*

$$\mathrm{Var}\,\mathcal{U}^* = \{\,\mathbf{u}_1 - \mathbf{u}_2 \in \mathrm{Var}\,\mathcal{U}^* \;:\mathbf{u}_1,\mathbf{u}_2 \in \mathrm{Kin}\,\mathcal{U}^*\,\}.$$

The corresponding Euler-Lagrange Equations for this obstacle inclusion results in the following boundary value problem

$$\begin{cases} -\,\mathrm{div}\,(\nu\;\nabla \mathbf{u}) - \mathbf{f} + \nabla p + \rho\;\nabla \mathbf{u}\,\mathbf{u} = 0, \quad in\;\Omega \\ \mathrm{div}\,(\mathbf{u}) = 0, \quad in\;\Omega \\ (\nu\;\nabla \mathbf{u} - p\,\mathbb{I})\;\mathbf{n} = 0, \quad on\;\partial\Omega_N \\ (\nu\;\nabla \mathbf{u} - p\,\mathbb{I})\;\mathbf{n} = \gamma_i, \quad on\;\Gamma_i \\ \mathbf{u} - \mathbf{u}_{slip} = 0, \quad on\;\Gamma_i \\ \mathbf{u} - \mathbf{u}_D = 0 \quad on\;\partial\Omega_D. \end{cases} \tag{5}$$

3.2 Variational equation for spinning obstructed fluid's flow

Here we the study the Magnus effect, described in Holzer and Sommerfeld (2009), which is the result of a non symmetric fluid flow condition produced when considering a spinning object embedded in a Poiseuille schematic flow. Figure 4 illustrates the proper context conditions to study the Magnus effect.

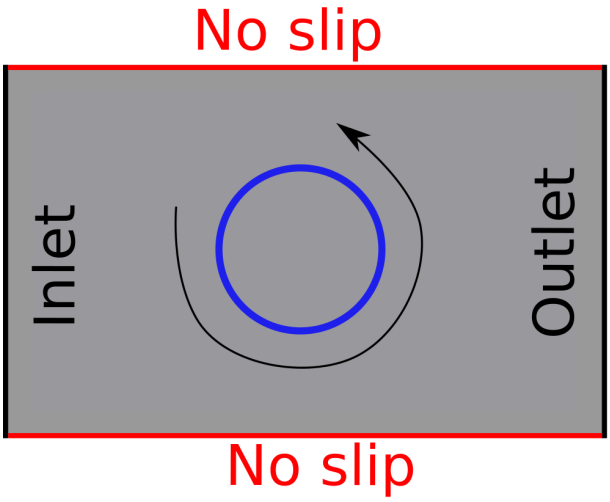

Figure 4: Representation of an circular spinning obstacle embedded in a rectangular channel.

Following the recent studies shown in Holzer and Sommerfeld (2009); Galindo-Torres (2013) and Shin et al. (2013), the Magnus effect still challenges the computational mechanics when modeling phenomena like soccer or baseball ball's distinct trajectories due to the combined translation and spinning. Since the obstacle is no longer fixed, rather it is spinning, the variational counterpart of Problem 3 must be updated.

Problem 4 (Navier Stokes equations with spinning obstacles constraints) *Given a regular domain Ω, a source function $\mathbf{f}$ defined on $\mathbf{L}^2(\Omega)$, find the velocity field denoted by $\mathbf{u}$, defined over the following manifold*

$$\mathrm{Kin}\,\mathcal{U}^* \equiv \{\mathbf{w} \in \mathbf{H}^1(\Omega) : \mathbf{w}|_{\partial\Omega_D} = \mathbf{u}_D\},$$

and find the Lagrangian multipliers p and γ_i defined on $L^2(\Omega)$ and $L^2(\Gamma^i)$ spaces, respectively, such that

$$\int_\Omega \nu\,(\nabla\mathbf{u};\nabla\mathbf{v})\;d\Omega - \int_\Omega (\mathbf{f};\mathbf{v})\;d\Omega - \int_\Omega \eta_p\;\mathrm{div}\,(\mathbf{u})\;d\Omega - \int_\Omega p\;\mathrm{div}\,(\mathbf{v})\;d\Omega$$
$$+ \int_\Omega \rho\;(\nabla\mathbf{u}\,\mathbf{u};\mathbf{v})\;d\Omega + \sum_i^N \int_\Gamma (\gamma_i;\mathbf{v}) + (\eta_{\gamma_i};\mathbf{u}-\mathbf{u}_{sp})\;\mathrm{d}\Gamma = 0,$$
$$\forall\,(\mathbf{v},\eta_p,\eta_{\gamma_i}) \in \left(\mathrm{Var}\,\mathcal{U}^*, L^2(\Omega), L^2(\Gamma^i)\right),$$

where the subspace $\mathrm{Var}\,\mathcal{U}^*$ is defined as

$$\mathrm{Var}\,\mathcal{U}^* = \{\,\mathbf{u}_1 - \mathbf{u}_2 \in \mathrm{Var}\,\mathcal{U}^* \;: \mathbf{u}_1, \mathbf{u}_2 \in \mathrm{Kin}\,\mathcal{U}^*\,\},$$

and where $\mathbf{u}_{sp}$ is defined in terms of an angular velocity α and obstacle radius R, that is

$$\mathbf{u}_{sp} = \begin{bmatrix} 0.0 & \alpha \\ -\alpha & 0.0 \end{bmatrix} \begin{bmatrix} R_x \\ R_y \end{bmatrix}.$$

The corresponding Euler-Lagrange Equations for this obstacle inclusion results in the following boundary value problem

$$\begin{cases} -\,\mathrm{div}\,(\nu\;\nabla\mathbf{u}) - \mathbf{f} + \nabla p + \rho\;\nabla\mathbf{u}\,\mathbf{u} = 0, \quad in\;\Omega \\ \mathrm{div}\,(\mathbf{u}) = 0, \quad in\;\Omega \\ (\nu\;\nabla\mathbf{u} - p\,\mathbb{I})\;\mathbf{n} = 0, \quad on\;\partial\Omega_N \\ (\nu\;\nabla\mathbf{u} - p\,\mathbb{I})\;\mathbf{n} = \gamma_i \quad on\;\Gamma_i \\ \mathbf{u} - \mathbf{u}_{sp} = 0, \quad on\;\Gamma_i \\ \mathbf{u} - \mathbf{u}_D = 0 \quad on\;\partial\Omega_D. \end{cases} \tag{6}$$

4 NUMERICAL METHODS

In the context of transport phenomena the Lattice Boltzmann model has been used extensively and successfully applied for more than 30 years, as shown in the research of He and Luo (1997); Chen and Doolen (1998). Given a set of particles, for a fixed time t, the particles inside the interval $\mathbf{r} + \delta\mathbf{r}$ whose velocity rank is bounded by $\mathbf{e} + \delta\mathbf{e}$ can be measured by using the distribution $f(\mathbf{r},\mathbf{e},t)$.

Velocity change ratio is often due to a force action over a limited time, then if the amount of particles does not changes through the time a balance expression can be written as

$$f(\mathbf{r} + \mathbf{e}\,\delta t, \mathbf{e} + \mathbf{F}\,\delta t, t + \delta t) - f(\mathbf{r},\mathbf{e},t) = 0. \tag{7}$$

For instantaneous interactions, such as particle collision, the balance is rewritten as

$$\frac{d[f(\mathbf{r},\mathbf{e},t)]}{dt} = \mathcal{Q}(f). \tag{8}$$

Thus, applying the chain rule in the previous equation, the *Lattice Boltzmann Equation* is achieved

$$\nabla f \cdot \mathbf{e} + \frac{\partial f}{\partial \mathbf{e}} \cdot \mathbf{F} + \frac{\partial f}{\partial t} = \mathcal{Q}(f). \tag{9}$$

In order to get a closed solution for Equation (9) the collision operator, represented by $\mathcal{Q}$, must be defined. The simplest method to write this collision operator is to consider an equilibrium distribution. Here, the *BGK* collision operator, described in Bhatnagar et al. (1954), is considered

$$\mathcal{Q}(f) = \omega \, \left(f^{eq} - f(\mathbf{r}, \mathbf{e}, t) \right), \tag{10}$$

where the ω coefficient measures the frequency of collisions. Furthermore, the *Equilibrium Distribution*[3] tunes and solves different physical scenarios. Replacing Equation (10) in Equation (9) the following equation is achieved

$$\nabla f \cdot \mathbf{e} + \frac{\partial f}{\partial \mathbf{e}} \cdot \mathbf{F} + \frac{\partial f}{\partial t} = \omega \, \left(f^{eq} - f \right). \tag{11}$$

The explicit solution for *Lattice Boltzmann* with BGK collision operator is given by

$$f(\mathbf{r} + \mathbf{e}\,\delta t, \mathbf{e} + \mathbf{F}\,\delta t, t + \delta t) = f(\mathbf{r}, \mathbf{e}, t) + \delta t\, \omega \, \left(f^{eq} - f(\mathbf{r}, \mathbf{e}, t) \right). \tag{12}$$

Neglecting external forces acting over the particles, Equation (12) takes the following expression, known as the *Lattice Boltzmann Method*:

$$f(\mathbf{r} + \mathbf{e}\,\delta t, t + \delta t) = f(\mathbf{r}, \mathbf{e}, t) + \delta t\, \omega \, \left(f^{eq} - f(\mathbf{r}, \mathbf{e}, t) \right). \tag{13}$$

For the numerical simulations we have employed the Lattice Boltzmann quasi incompressible scheme given by the D2Q9 model, as proposed by He and Luo (1997).

5 BOUNDARY CONDITIONS IMPOSITION

As shown in Problems 3 and 4 the variational foundations allowed to obtain the complete set of *Euler-Lagrange* equations. As described in Section 2, every compatible load is characterized by this procedure. In this context, Lagrangian multipliers are responsible to enforce a kinematic constraint. Therefore, to take into account boundary conditions for Problems 3 and 4, the Lattice Boltzmann Equation (13) must be updated as

$$f(\mathbf{r} + \mathbf{e}\,\delta t, t + \delta t) = f(\mathbf{r}, \mathbf{e}, t) + \delta t\, \omega \, \left(f^{eq} - f(\mathbf{r}, \mathbf{e}, t) \right) + S(\mathbf{r}, t). \tag{14}$$

The extra term $S(\mathbf{r}, t)$ is generally used to represent external forces, as shown schematically in Figure 5. We note that there is a certain flexibility when tunning this term. Here it is assumed that a volumetric force[4] $\mathbf{F}(\mathbf{r}, t)$ can be applied in each Lattice array and the following expression, based on Mohamad and Kuzmin (2010), will be used

$$S(\mathbf{r}, t) = \frac{\delta\, t}{v} \, \left(w\, \mathbf{e}; \mathbf{F}(\mathbf{r}, t) \right), \tag{15}$$

where w denotes the $w_i - eth$ different weight directions. It can be concluded from the previous expression that the source term does not add or subtract mass and it provides, at each time step, a momentum such that the Lattice array is perturbed with a finite impulse, which is given by

$$\left(S(\mathbf{r}, t); v\, \mathbf{e} \right) = \left(\frac{\delta\, t}{v} \, \left(w\, \mathbf{e}; \mathbf{F}(\mathbf{r}, t) \right); v\, \mathbf{e} \right) = \mathbf{F}(\mathbf{r}, t)\, \delta t.$$

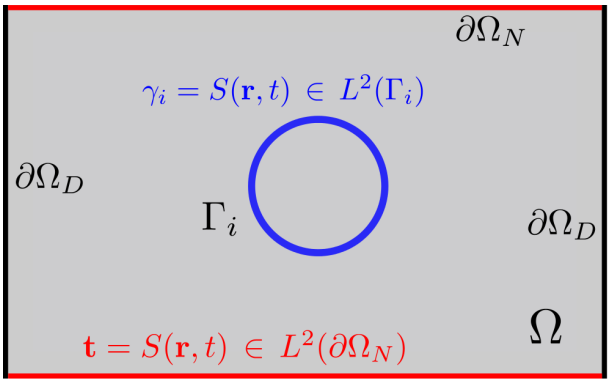

Figure 5: Employed technique to impose *Force type* boundary conditions.

As mentioned before, the boundary conditions and extra forces are imposed employing extra source loads as represented by Equation (15) and described in Mohamad and Kuzmin (2010). Regarding the computational implementation, these forces are effectively applied following a standard relaxation scheme:

$$S(\mathbf{r},t) = C_p \left\| \mathbf{u}_g(\mathbf{r},t) - \mathbf{u}(\mathbf{r},t) \right\| + C_I \sum_i \left\| \mathbf{u}_g(\mathbf{r},t_i) - \mathbf{u}(\mathbf{r},t_i) \right\| \Delta t_i, \tag{16}$$

where $\mathbf{u}_g(\mathbf{r},t)$ represents a known velocity, C_p and C_I are relaxation coefficients, often denoted as proportional and integral controllers. Here it is important to note that Equation (16) is satisfied for every *Spin or No slip* boundary constraints. The relaxation coefficients are described in Table 1.

Magnitude	Numerical domains Ω	Numerical boundaries $\partial\Omega$, Γ
$\mathbf{u}$	$C_p = 1.0E-04$, $C_I = 1.0E-06$	$C_p = 7.0E-05$, $C_I = 7.0E-08$
$\nabla\mathbf{u}$	$C_p = 1.0E-05$, $C_I = 1.0E-08$	

Table 1: Order of magnitude used for the relaxation coefficients.

6 NUMERICAL EXPERIMENT 1

In the first experiment a square channel with a planar shield inclusion is considered, see Figure 6. The simulation parameters are properly defined in Table 2. This simulation attempts to show a methodology to establish the numerical evaluation of the force that the fluid exert to the obstacle.

[3]Also known as *Maxwell Boltzmann* distribution.
[4]Without loss of generality these volumetric forces are the Lagrangian multipliers.

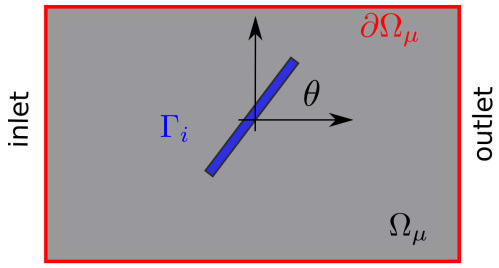

Figure 6: Planar shield's inclusion in rectangular channel.

Parameter	Symbol	Value
Reynolds number	R_E	20.0
Domain size	$N_x \times N_y$	50×50
Obstacle length	l	10
Obstacle localization	$(I_x; I_y)$	$(25; 25)$
Inlet Velocity profile	$(u_x; u_y)$	$(0.10; 0)$
Maximum Shield rotation	θ_{max}	$0.5\,\pi$
Obstacle's Boundary Condition	-	No slip

Table 2: Simulation parameters for experiment 1.

To illustrate the performance of the LBM the results at a particular shield orientation $\theta = 0.25\,\pi$ are presented. The velocity magnitude is shown in Figure 7(a) and the acceleration field that influences the obstacle is shown in Figure 7(b). The corresponding Lagrangian multiplier, which enforces the no slip boundary constraint for the obstacle is shown in Figure 7(c). Finally, Figure 7(d) shows the density variations due to the inclusion of this planar obstruction.

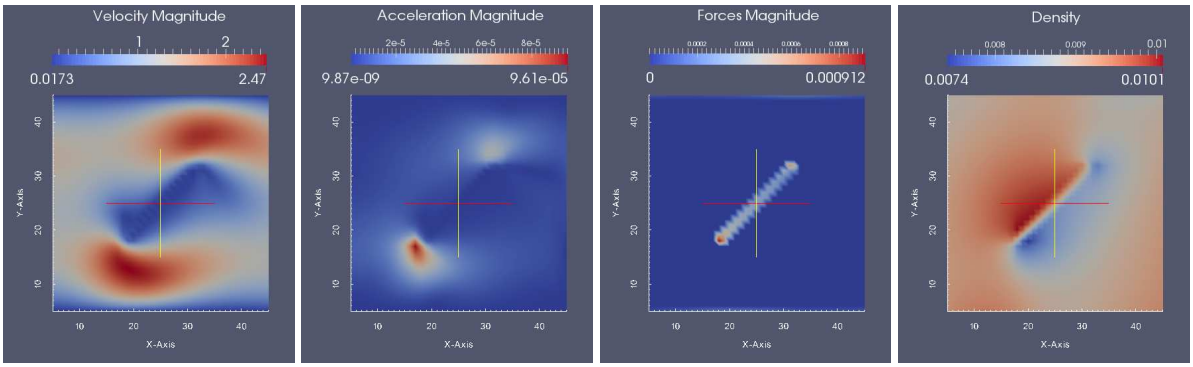

(a) $\|\mathbf{u}\|$ (b) $\|\mathbf{a}\|$ (c) $\|\gamma\|$ (d) ρ

Figure 7: Solution profiles for experiment 1 using parameters of Table 2 at $\theta = 0.25\,\pi$.

To complete the analysis we carried out simulations varying θ from 0 to $\pi/2$ in order to shows the corresponding variations of obstacle forces, as shown in Figure 8.

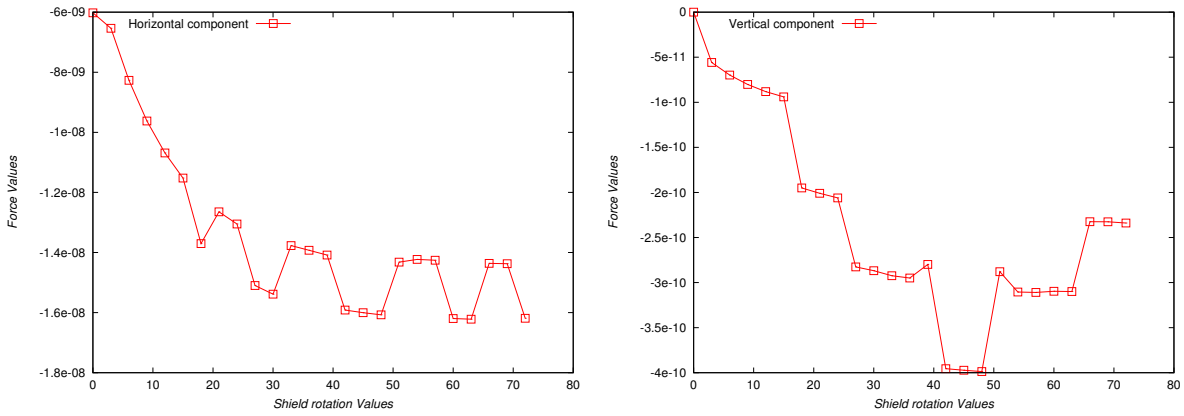

(a) γ_x component (b) γ_y component

Figure 8: Force sensitivity due to rotations of θ from 0 to $\pi/2$.

7 NUMERICAL EXPERIMENT 2

Here, a square channel with a spinning circular inclusion is considered, as described by Figure 4. The simulation parameters are defined in Table 3. This simulation attempts to show a methodology to establish the numerical evaluation of the force that the fluid exerts to the spinning obstacle.

Parameter	Symbol	Value
Domain size	$N_x \times N_y$	100×100
Obstacle Radius	R	10
Obstacle localization	$(I_x; I_y)$	$(40; 50)$
Reynolds number	R_E	20.0
Inlet Velocity profile	$(u_x; u_y)$	$(0.03; 0.0)$
Obstacle's Angular velocity	α	-0.005
Obstacle's Boundary Condition	-	Spin

Table 3: Simulation parameters for experiment 2.

To illustrate the performance of the Lattice Boltzmann Method, the results for velocity magnitude are shown in Figure 9(a), the acceleration field that influences the obstacle is shown in Figure 9(b). The corresponding Lagrangian multiplier, which enforces the spinning boundary constraint for the obstacle is shown in Figure 9(c). To conclude the set of results, Figure 9(d) shows the density variations due to the inclusion of this circular spinning obstruction.

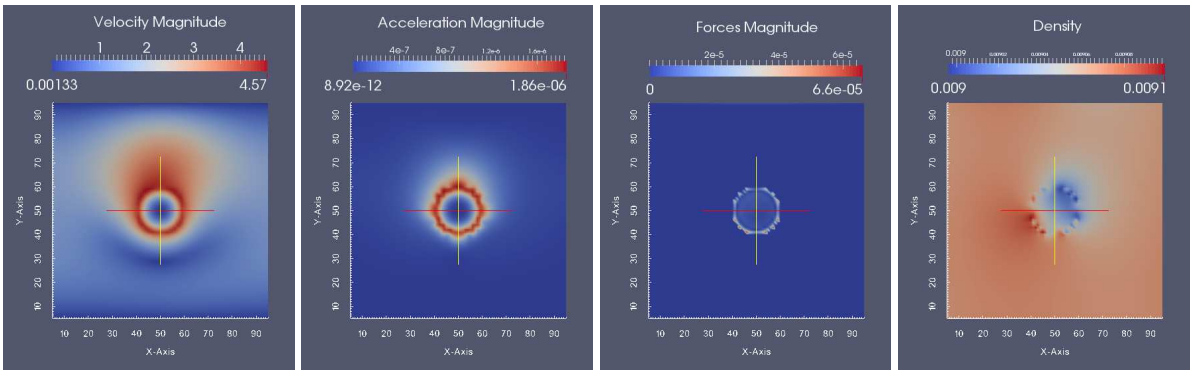

(a) $\|\mathbf{u}\|$ (b) $\|\mathbf{a}\|$ (c) $\|\gamma\|$ (d) ρ

Figure 9: Solution profiles for experiment 2 using parameters of Table 3.

8 CONCLUSIONS

In this work we showed a modeling methodology based in the *Principle of virtual power balance* which allowed to generate a meaningful variational framework for modeling viscous flows phenomena. The developed *Euler-Lagrange* equations were successfully implemented using the Lattice Boltzmann Method.

Among the Euler-Lagrange equations, the *no slip* and *spin* boundary constraints were naturally obtained from the variational framework. Recalling that the boundary constraints differs from boundary conditions as *Dirichlet or Neumann* in the fact that Lagrangian multipliers were employed to modify the functional, by relaxing the constraints from the kinematic admissible manifolds.

The LBM implementation recovers the incompressible Navier Stokes equations when considering the presence of obstacles which were established as fixed or characterized by a motion action. Every solution field was plotted at steady state. In despite of the fact that we have not shown transient effects, the Lattice Boltzmann Method is in it self a transient solver, the steady state for every simulation was defined employing the following criteria

$$\frac{\|\mathbf{u}_{t+i} - \mathbf{u}_t\|_\infty}{\|\mathbf{u}_t\|_\infty} \leq tolerance,$$

where t is a generic time step.

The results were obtained when modeling specific challenging physical situations. The self consistent modeling procedures allows to obtain piecewise Euler-Lagrange equations, which were included in the numerical solver based in the Lattice Boltzmann Method. The computed solutions responds with significant accuracy, when compared with the expected behavior for the analyzed situations.

ACKNOWLEDGEMENT

The authors would like to thank the resources provided by the Brazilian research council CAPES and FAPEMIG.

REFERENCES

Artoli A.M., Kandhai D., Hoefsloot H.C.J., Hoekstra A.G., and Sloot P.M.A. Lattice BGK simulations of flow in a symmetric bifurcation. *Future Generation Computer Systems*, 20(6 SPEC. ISS.):909–916, 2004. ISSN 0167739X. doi:10.1016/j.future.2003.12.002.

Bhatnagar P.L., Gross E.P., and Krook M. A model for collision processes in gases. i. small amplitude processes in charged and neutral one-component systems. *Phys. Rev.*, 94:511–525, 1954. doi:10.1103/PhysRev.94.511.

Chen S. and Doolen G.D. Lattice Boltzmann Method for Fluid Flows. *Annual Review of Fluid Mechanics*, 30(1):329–364, 1998. ISSN 0066-4189. doi:10.1146/annurev.fluid.30.1.329.

Freund J.B. Numerical Simulation of Flowing Blood Cells. *Annual Review of Fluid Mechanics*, 46(1):67–95, 2014. ISSN 0066-4189. doi:10.1146/annurev-fluid-010313-141349.

Galindo-Torres S.A. A coupled Discrete Element Lattice Boltzmann Method for the simulation of fluid-solid interaction with particles of general shapes. *Computer Methods in Applied Mechanics and Engineering*, 265:107–119, 2013. ISSN 00457825. doi:10.1016/j.cma.2013.06.004.

Germain P. On the method of virtual power in continuum mechanics. *SIAM Journal on Applied Mathematics*, 25(3):556–575, 1973. ISSN 1559-3959. doi:10.2140/jomms.2009.4.281.

Golbert D.R., Blanco P.J., Clausse a., and Feijóo R.a. Tuning a lattice-Boltzmann model for applications in computational hemodynamics. *Medical Engineering and Physics*, 34(3):339–349, 2012. ISSN 13504533. doi:10.1016/j.medengphy.2011.07.023.

He X. and Luo L.S. Lattice Boltzmann Model for the Incompressible Navier–Stokes Equation. *Journal of Statistical Physics*, 88(3/4):927–944, 1997. ISSN 0022-4715. doi:10.1023/B:JOSS.0000015179.12689.e4.

Holzer A. and Sommerfeld M. Lattice Boltzmann simulations to determine drag, lift and torque acting on non-spherical particles. *Computers and Fluids*, 38(3):572–589, 2009. ISSN 00457930. doi:10.1016/j.compfluid.2008.06.001.

Maugin G.a. The method of virtual power in continuum mechanics: Application to coupled fields. *Acta Mechanica*, 35(1-2):1–70, 1980. ISSN 00015970. doi:10.1007/BF01190057.

Mohamad A. and Kuzmin A. A critical evaluation of force term in lattice Boltzmann method, natural convection problem. *International Journal of Heat and Mass Transfer*, 53(5-6):990–996, 2010. ISSN 00179310. doi:10.1016/j.ijheatmasstransfer.2009.11.014.

Shin J., Lee J., and Lee S. A strain-rate model for a lattice Boltzmann BGK model in fluid-structure interactions. *Computers and Fluids*, 88:126–135, 2013. ISSN 00457930. doi:10.1016/j.compfluid.2013.08.009.

Taroco E.O., Feijóo G.R., Blanco P.J., and Feijóo R.A. *Introducción a la Formulación Variacional de la Mecánica*. LNCC Internal Reports, 2014.